AD-A051 335 MCDONNELL DOUGLAS ASTRONAUTICS CO HUNTINGTON BEACH CALIF F/G 4/1
A QUANTITATIVE MODEL OF IONOSPHERIC ELECTRON DENSITY.(U)
FEB 78 W P OLSON, K A PFITZER N00014-75-C-0821
UNCLASSIFIED MDC-G7433 NL

1 OF 1
ADA
051335

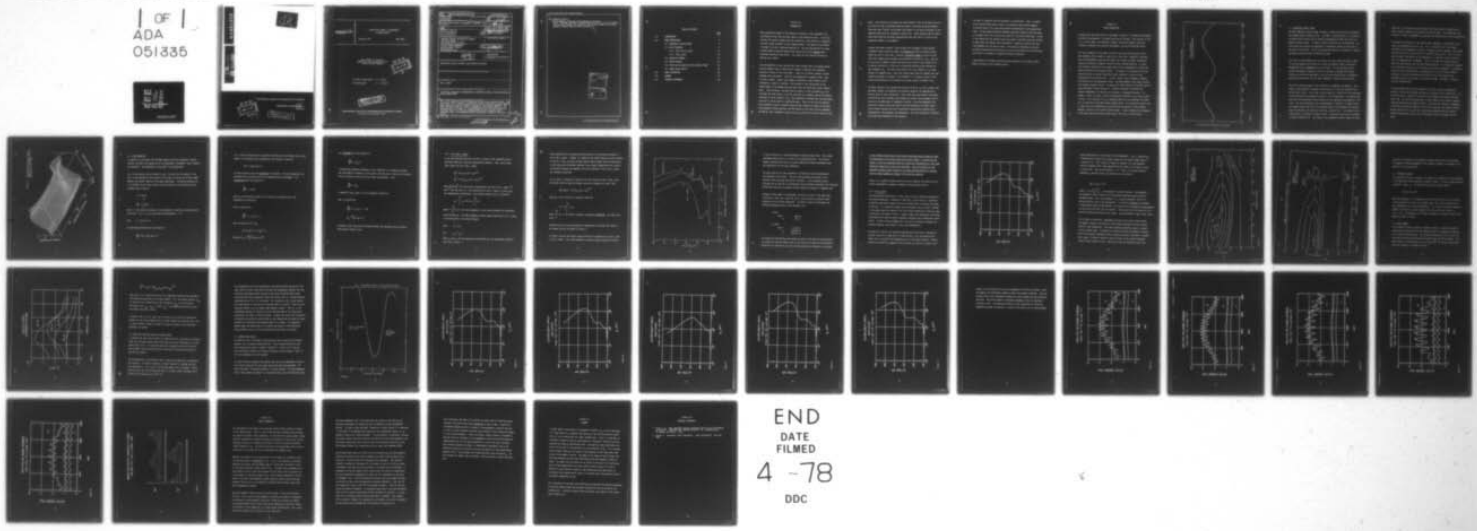

END
DATE
FILMED
4 -78
DDC

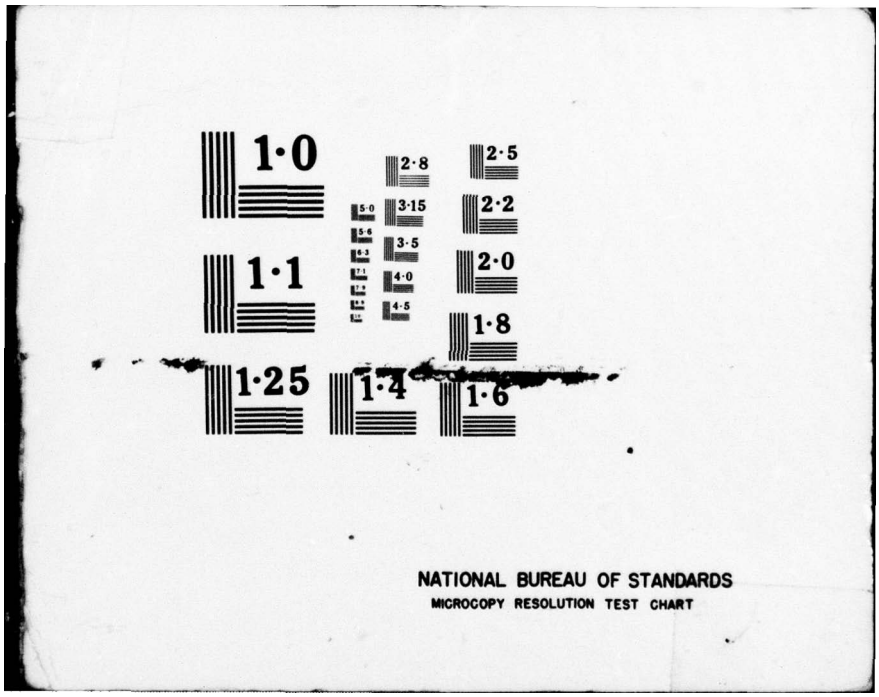
1·0
1·1
1·25
1·4
1·6
1·8
2·0
2·2
2·5
2·8
3·15
3·5
4·0
4·5
5·0
NATIONAL BUREAU OF STANDARDS
MICROCOPY RESOLUTION TEST CHART

12

MCDONNELL DOUGLAS ASTRONAUTICS COMPANY

MCDONNELL DOUGLAS CORPORATION

MCDONNELL DOUGLAS

A QUANTITATIVE MODEL OF IONOSPHERIC ELECTRON DENSITY

February 1978

MDC G7433

Final Report for Contract
N00014-75-C-0821 Sponsored by the
Office of Naval Research

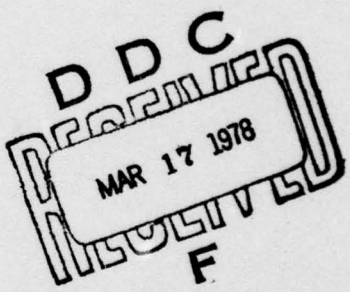

Principal Investigator: W. P. Olson

Co-Investigator: K. A. Pfitzer

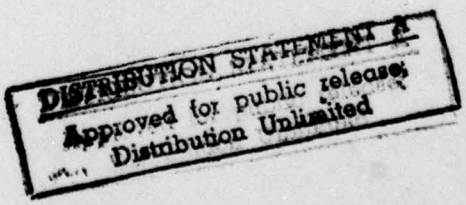

MCDONNELL DOUGLAS ASTRONAUTICS COMPANY-WEST

5301 Bolsa Avenue, Huntington Beach, CA 92647

SECURITY CLASSIFICATION OF THIS PAGE *(When Data Entered)*

(14) **REPORT DOCUMENTATION PAGE**

READ INSTRUCTIONS BEFORE COMPLETING FORM

1. REPORT NUMBER: MDC-G7433
2. GOVT ACCESSION NO.
3. RECIPIENT'S CATALOG NUMBER

(9) rept.

4. TITLE (and Subtitle): A Quantitative Model of Ionospheric Electron Density.
5. TYPE OF REPORT & PERIOD COVERED: Final 2/75 - 2/78
6. PERFORMING ORG. REPORT NUMBER: Feb 75 - Feb 78

(10)

7. AUTHOR(s): Willard P. Olson, Karl A. Pfitzer
8. CONTRACT OR GRANT NUMBER(s): (15) N00014-75-C-0821

9. PERFORMING ORGANIZATION NAME AND ADDRESS
McDonnell Douglas Astronautics Company
5301 Bolsa Avenue
Huntington Beach, CA 92647

10. PROGRAM ELEMENT, PROJECT, TASK AREA & WORK UNIT NUMBERS

11. CONTROLLING OFFICE NAME AND ADDRESS
Office of Naval Research
Ballston Center Tower #1
800 N. Quincy
Arlington, VA 22217

(11)

12. REPORT DATE: 28 February 1978
13. NUMBER OF PAGES: 42

14. MONITORING AGENCY NAME & ADDRESS *(if different from Controlling Office)*

(12) 47 p.

15. SECURITY CLASS. *(of this report)*: UNCLASSIFIED
15a. DECLASSIFICATION/DOWNGRADING SCHEDULE

16. DISTRIBUTION STATEMENT *(of this Report)*

Approved for public release, distribution unlimited.

17. DISTRIBUTION STATEMENT *(of the abstract entered in Block 20, if different from Report)*

18. SUPPLEMENTARY NOTES

Tech., other

19. KEY WORDS *(Continue on reverse side if necessary and identify by block number)*

Ionosphere, Atmosphere, Magnetosphere, Quantitative Models, Electron Density, Radio Communication

20. ABSTRACT *(Continue on reverse side if necessary and identify by block number)*

This report summarizes work performed during the entire contract period. The general goal was to develop a quantitative global ionospheric electron density model that can be used to predict variations in the electron density. The model developed under this contract represents the electron density at all latitudes and local times, it is computationally fast and can be used in a predictive mode. The electron density model relies on physical input parameters that can be measured directly (intensity of bands of the solar

→ next page (over)

DD FORM 1 JAN 73 1473 EDITION OF 1 NOV 65 IS OBSOLETE

SECURITY CLASSIFICATION OF THIS PAGE *(When Data Entered)*

389310

20. ABSTRACT (Cont'd)
electromagnetic spectrum and the density of the solar wind). The model features include structure of the E, F_1, and F_2 layers, the day-night changes, the equatorial and seasonal anomalies and dependences on several forms of solar variability.

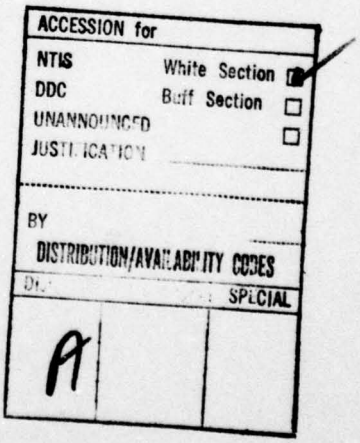

TABLE OF CONTENTS

Section 1.0

INTRODUCTION

Most quantitative models of the density of electrons in the ionosphere, N_e, constructed to date have not been usable in the predictive sense. It has been realized for several decades that the variability in the density of ionospheric electrons causes problems in radio communications. The nature of the problem is thought to be well understood physically. Thus the availability of a quantitative model of electron density that can be used to help predict these variations should be quite useful. The intent of this contract has been to develop such a model.

From the beginning it was realized that there already were in existence several physical models--that is, models which attempt to describe the ionosphere entirely in terms of first principles. There are at present, however, several problems with such models. They are very cumbersome as computer codes. None of them is global. Rather they attempt to describe a single feature of the ionosphere or region in latitude. The attitude in the construction of the present model was to demand from the outset that the model meet several requirements. These included: the model must be global--it must represent N_e at all latitudes and local times, it must be very fast as a computer code yet accurately represent all gross features in N_e. Most important, the model must be constructed such that it can be used in a predictive mode. Thus, it must rely on physical input parameters that are directly measured (the intensity of bands of the solar electromagnetic energy spectrum and the density of the solar wind are examples). This implies that "secondary" indices such as K_p would not be used as inputs to the

model. Such indices are averaged over long periods of time (a few hours) and are the result of many interrelated physical events in the near earth environment. There are other "inputs" to the model that appear in the form of constants in the equations describing the ionospheric layers, etc. These constants must be determined from satellite and other observational data sets (the "L" value for the equatorial anomaly is an example).

A model with these "primary" (time varying) and "secondary" (fixed program constants) inputs should be capable of predicting N_e when the proper primary inputs are used in real time. Currently statistical models are used to help with radio communication problems associated with variability in N_e. They can be used only to suggest seasonal and solar cycle trends in the variability in N_e and are therefore of little use in predicting the day-to-day and hour-to-hour changes in N_e. This short term variability in N_e, however, is of great concern for communications. While the present model does not address such fine structure problems as "spread F" and "sporadic E" it should be useful in the study and prediction of the variability of gross spatial structures in N_e.

The model features in N_e include the structure of the E, F_1, and F_2 layers, the day-night changes, the equatorial and seasonal anomalies and dependences on several forms of solar variability. Thus, solar cycle and seasonal variations find their way into the model both through its primary input parameters and in the use of the MDAC model of atmospheric density. Both electromagnetic and corpuscular energy sources are used to provide information for model inputs. This inclusion required the use of coordinate transormations between solar-magnetospheric and geographic and geomagnetic. Very fast analytical transformation codes were developed for this purpose.

The model is complete with the exception of "calibration." Thus, it remains to use observational data as input to the computer code and then compare calculated values of N_e with those obtained from ionograms at the appropriate times. We have agreed with Naval Research Laboratory personnel that the month of September 1977 will be used as the epoch for the primary data base. It was in this month that the current solar cycle began in earnest--there are periods of both quiet and moderate solar disturbance. Hopefully, several data sets from SOLRAD-HI will be used as input. The necessary ionograms are not yet available from the World Data Center, but we are told there will be sufficient data within a few months to complete the model calibration.

A description of the model construction and computation of N_e based on the model are given in the following section.

Section 2.0

MODEL DESCRIPTION

We report here the construction of the model in terms of its primary and secondary constants and parameters. The model specifically includes: the structure of the E, F_1, and F_2 layers, the equatorial anomaly, the winter anomaly, polar cap structure, semiannual and seasonal dependences, and the mid-latitude trough.

The input parameters to the model are chosen such that satellite data can be used together with the model to specify N_e in real time. Hopefully, with data from the HELIOCENTRIC satellite, the model can be used to predict ionospheric features controlled by magnetic fields and solar charged particles. In part, the predictive capability of the model stems from its dependence on inputs from other quantitative environmental models. For example, the location of the mid-latitude trough is largely controlled by the locations (L values) of the plasmapause and the auroral oval. In fact, several gross ionospheric features are controlled by the geomagnetic field. The MDAC magnetic field model provides the necessary magnetic inputs. The model also relies heavily on the MDAC model of upper atmospheric neutral density, N. Several ionospheric structures and temporal dependences tie directly to variations in atmospheric density. An example is shown in Figure 1 where the semiannual variation in N_e at the F_2 peak is shown. This variation in N_e is produced entirely by the semiannual variation in N as described by the MDAC neutral density model. The structures of the E and F_1 layers are also determined by calculating the absorption of solar electromagnetic radiation in the neutral density model. A short summary of the features of the MDAC atmospheric density model used in this study is given below.

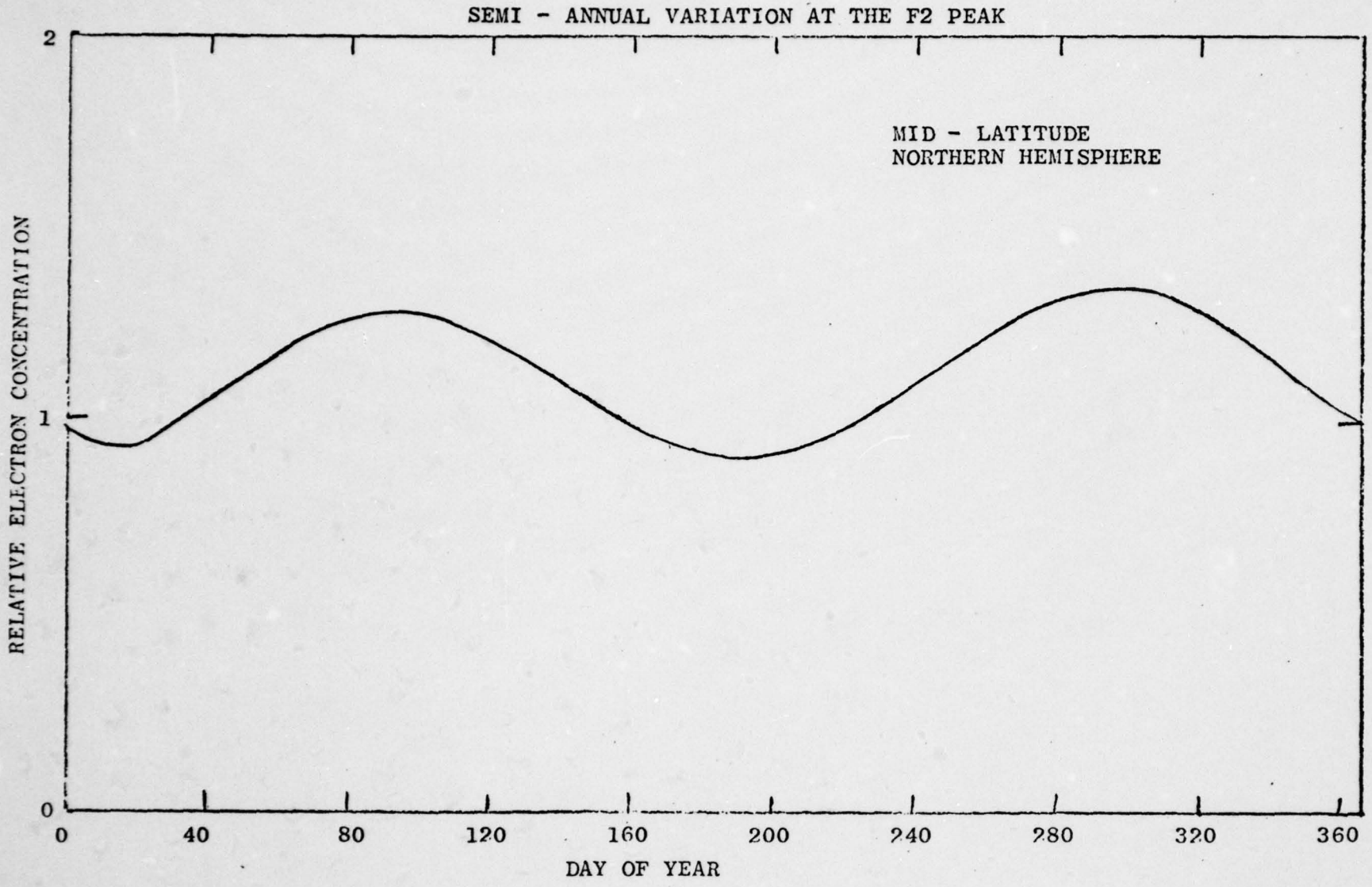
SEMI - ANNUAL VARIATION AT THE F2 PEAK
MID - LATITUDE
NORTHERN HEMISPHERE
RELATIVE ELECTRON CONCENTRATION
2
1
0
0
40
80
120
160
200
240
280
320
360
DAY OF YEAR

Figure 1.

2.1 ATMOSPHERIC DENSITY MODEL

The MDAC atmospheric density model includes as inputs both the solar ultraviolet and charged particle energy sources. The model is semi-empirical--it is based on available satellite data and our present understanding of both the UV and corpuscular energy sources. It offers a global description of the atmosphere. The model takes into account the dependence of atmospheric density on the value of the solar flux constant. The UV and corpuscular effects are computed in separate coordinate systms and their contributions added.

Ever since an accelerometer was first flown on a polar satellite (Bruce, 1968), it has been apparent that there are at least two density bulges in the lower thermosphere during geomagnetically quiet times. The low-latitude bulge is usually attributed to heating by solar UV radiation (although other energy sources may contribute importantly), but the high-latitude bulge is produced by particles precipitating into the upper atmosphere through the dayside cusps.

The solar UV heating source is best described in geographic coordinates. Thus, inputs to the atmospheric computer subroutine must include the universal time and the time of year. Local time is also entered as a function of the coordinates of the point where the atmospheric density is to be determined. The dayside cusp particles are constrained to precipitate into the atmosphere along magnetic field lines. The cusp intersection with the atmosphere is nominally 15 degrees below the magnetic dipole axis with its longitude center on the magnetic noon meridian plane as defined by the dipole axis and the sun-earth line. The extent of this intersection in longitude is about 12 hours. The extent of the cusp in latitude is several degrees (3-5). The region of the atmosphere actually heated by these

particles is of course much larger because the impact energy is spread out by winds, thermal conduction, and possibly by gravity waves. The corpuscular contribution is found in geomagnetic coordinates and combined with the UV contribution.

This model of the density of the neutral upper atmosphere is functionally very simple and computationally very fast. Yet, it describes most of the known variations in the atmosphere; latitude, longitude, diurnal, seasonal, semi-annual, altitude, solar cycle and variations in particle precipitation. Thus it can be used to predict the density of the atmosphere as a function of time, position, solar and magnetospheric parameters. Since it includes the heating effect of particles precipitating into the high latitude regions, it is especially valuable in the study and prediction of the density of the polar atmosphere. Furthermore, since this high latitude effect is parameterized, it can be used to predict increases in the high latitude density when the solar wind particle flux increases and the cusp location is observed to change. The model is analytic and thus differentiable.

The three dimensional mercator projection in Figure 2 shows the atmospheric density at 400 km during summer solstice at a universal time of 1600 hours. The UV density peak is located to the north of the equator and at about 1400 hours local time. The particle heating peak is most intense on the subsolar magnetic longitude containing the magnetic dipole. Since the total density is dependent on the particle heating effect as well as the UV heating, the northern particle heating peak which is in sunlight is much more pronounced than the southern particle heating peak which is far into darkness during the summer solstice night.

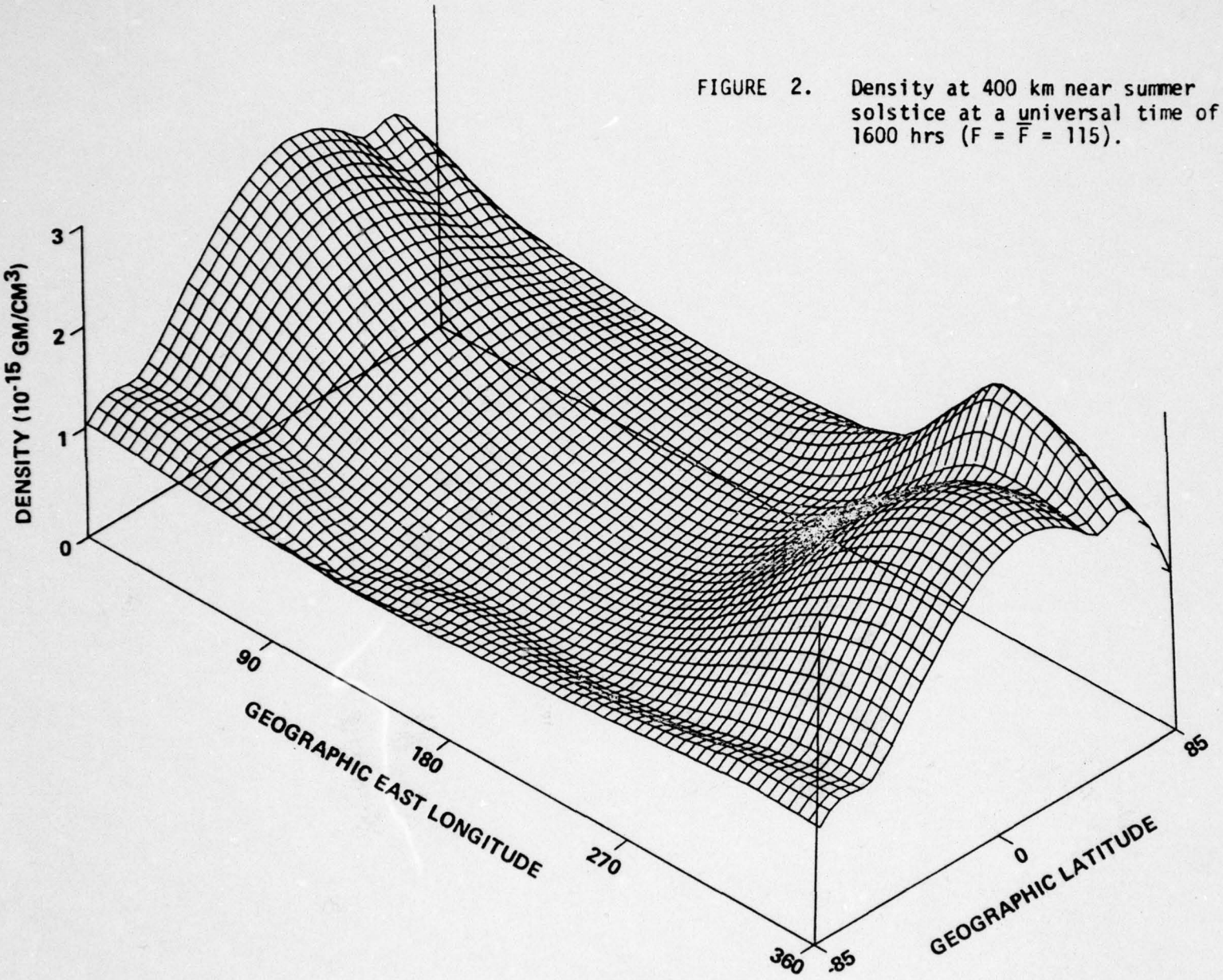

FIGURE 2. Density at 400 km near summer solstice at a universal time of 1600 hrs ($F = \bar{F} = 115$).

2.2 LAYER FORMATION

In addition to the inputs from the MDAC magnetic field and atmospheric neutral density, the model of N_e makes use of our knowledge of ionospheric layer formation and anomalies. The formulation of the model is discussed below.

Let S be the energy flux at location ℓ and S + dS the flux at location $\ell + d\ell$. Let σ be the absorption cross section of the atoms of the gas and N their number density (the neutral density of the upper atmosphere). The energy absorbed, dS, in a cylinder of unit cross section and axis parallel to the direction of the incident beam is given by

$$dS = S\sigma N \, d\ell$$

$$\frac{dS}{S} = \sigma \int_{\infty}^{\ell_0} N d\ell = -\tau$$

where τ is the optical thickness of the atmosphere at location ℓ_0 along the path to the sun. As $S \to S_\infty$ (its value above the atmosphere) $\tau \to 0$.

Thus $S = S_\infty \exp(-\tau)$,

and the energy absorbed per unit volume is

$$\frac{dS}{d\ell} = N\sigma S = N\sigma S_\infty \exp(-\tau).$$

If η is the ion/electron pair production efficiency per unit energy, then q (the number if ion/electron pairs produced per unit volume) is given by

$$q(\ell) = N\sigma\eta S_\infty \exp(-\tau).$$

The above equation gives the <u>production</u> of electrons. The two predominant loss mechanisms for ion/electron pairs are recombination and attachment. For <u>recombination</u> the loss equation is

$$\frac{dN_e}{dt} = -\alpha N_e N^+$$

where N_e is the electron density N^+ the positive ion density and α the recombination coefficient.

Thus, at equilibrium

$$\frac{dN_e}{dt} = q - \alpha N_e N^+ = 0$$

Then, assuming that $N^+ \approx N_e$,

$$N\sigma\eta S_\infty \exp(-\tau) - \alpha N_e^2 = 0$$

Therefore, $N_e = \left[\frac{N\sigma\eta S_\infty}{\alpha} \exp(-\tau)\right]^{1/2}$

For attachment the loss equation is

$$\frac{dN_e}{dt} = -b\, N_e\, N$$

In discussing attachment processes in the ionosphere it is generally assumed that the number of neutrals is much greater than the ions so that when ionization occurs the neutral density does not change significantly. Thus

$$\frac{dN_e}{dt} = -\beta\, N_e$$

is generally used, where β is the attachment coefficient.

Then, at equilibrium

$$\frac{dN_e}{dt} = q - \beta\, N_e = 0 \quad \text{and}$$

$$N_e = \frac{N\sigma\eta_\infty}{\beta} \exp(-\tau)$$

In general α and β may vary with height because the reactions usually involve three bodies instead of two.

2.2.1 The E and F_1 Layers

It has been observed that the E and the F_1 layers of the ionosphere can be described quite well using the recombination equation. Thus, using simple layer theory for the E and F_1 layers

$$N_e^E = [N\, S_E\, \alpha_E \exp(-\tau_E)]^{1/2}$$

$$N_e^{F_1} = [N\, S_{F_1}\, \alpha_{F_1} \exp(-\tau_{F_1})]^{1/2}$$

where N_e^E and $N_e^{F_1}$ are the electron concentrations for the E and F_1 layers, S^E and S^{F_1} are the solar U.V. flux affecting the E and F_1 layers, α_E and α_{F_1} are the recombination coefficients, N the neutral density, and τ_E is given by

$$\tau_E = \int_{\infty}^{\ell_o} \sigma_E\, N\, d\ell \approx \sigma_E \int_{\infty}^{\ell_o} N\, d\ell$$

where $T \equiv \int_{\infty}^{\ell_o} N\, d\ell$ is the total atmospheric cross section between the observation point and the sun. The MDAC atmospheric density model (described in 2.1) is used in the evaluation of the above integral.

Then $\tau_E = \sigma_E\, T$

and $\tau_{F_1} = \sigma_{F_1}\, T$

where σ_E and σ_{F_1} are the absorption coefficients for the wavelengths affecting the E and F_1 layers.

These equations give an approximate description of the observed structures in the E and F_1 layers. Changes in T depend on the neutral density and the location of the sun. Thus, by using the MDAC neutral density model (which contains most of the large scale variations observed in the neutral atmosphere) and a simple sun-position program, the temporal variations observed in the E and F_1 layers are accurately described.

The F_1 layer is essentially turned off at local sunset but the E layer, while diminished from its daytime strength, persists throughout the night. Thus

$$N_e^E \text{ (night)} = [N S_E' \alpha_E \exp(-\tau_E')]^{1/2}$$

where S_E' is the intensity of scattered light and

$$\tau_E' = \sigma_E \int_{\infty}^{\ell_o} N \, d\ell$$

where $\int_{\infty}^{\ell_o} N \, d\ell$ is the optical thickness (integrated <u>vertically</u> - not toward the sun).

Profiles of N_e at noon and midnight as represented by the model are shown at the equator and mid latitudes in Figure 3.

In Figure 3 we note the rather large unrealistic dip between the E and F_1, and F_1 and F_2 layers. This large decrease in electron density between the layers

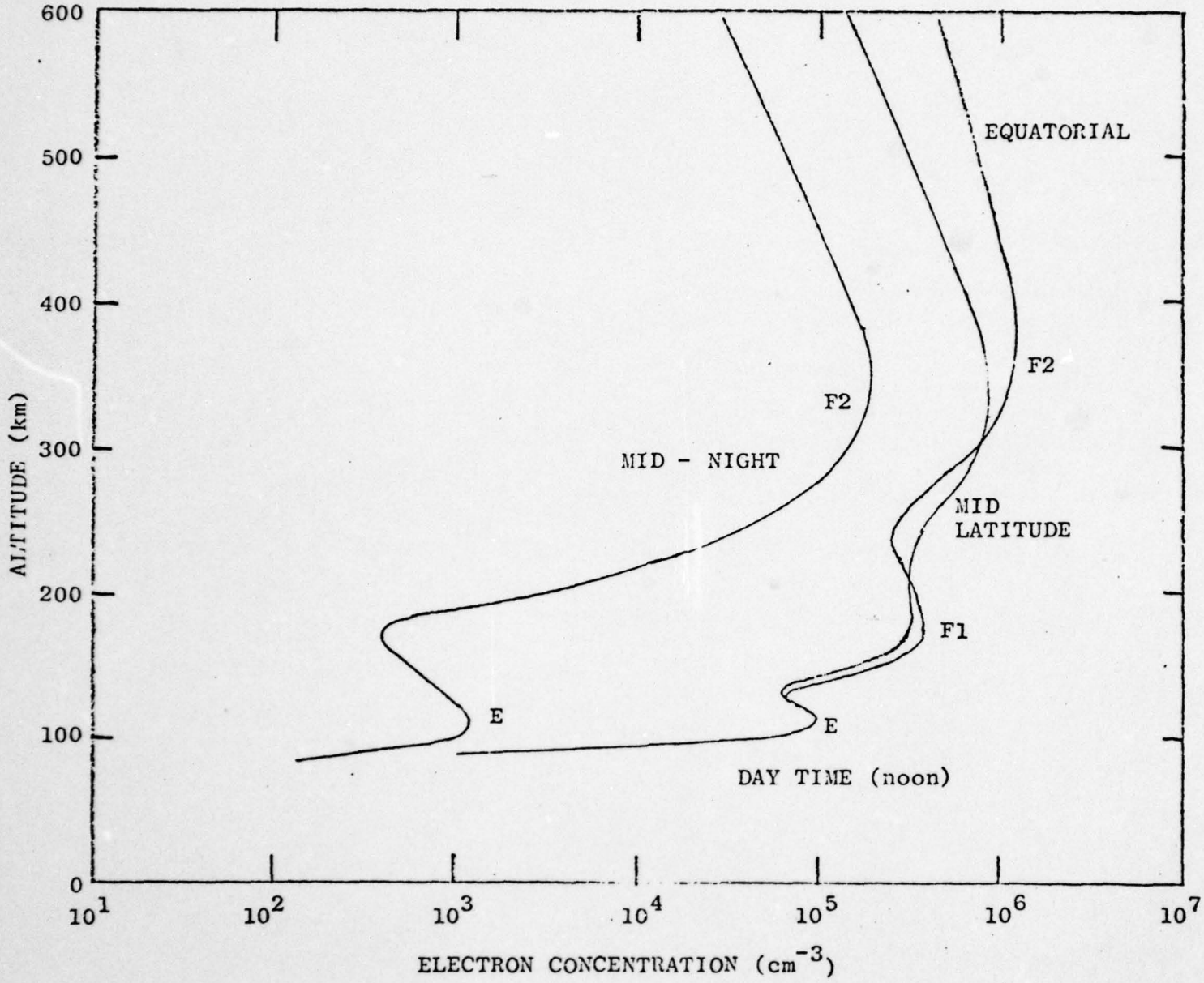
600
500
400
300
200
100
0
ALTITUDE (km)
EQUATORIAL
F2
F2
MID - NIGHT
MID
LATITUDE
F1
E
E
DAY TIME (noon)
10^1
10^2
10^3
10^4
10^5
10^6
10^7
ELECTRON CONCENTRATION (cm^{-3})

Figure 3.

is due to the use of a single wavelength to describe each layer. This single wavelength description is, of course, an oversimplification. The electromagnetic spectrum from the sun is quite complex and several wavelength bands are responsible for the layer formations.

The above analysis has been expended to include more than one wavelength in the formation of the layers. The only time consuming calculation is the integral which calculates the optical thickness. This calculated optical thickness can be used for all wavelengths having different absorption and ionization coefficients and source strengths without extensive increases in computer time.

Although a large number of wavelengths can easily be used, it was found that 2 terms for E layer and 3 terms for the F_1 layer provide an excellent representation of the altitude dependence. The model currently incorporates the following wavelength bands in the parameter list.

E Layer

Term 1	1026 °A
2	977 °A

F_1 Layer

Term 1	10-170 °A
2	170-796 °A
3	796-911 °A

The absorption coefficients associated with each of the bands has been adjusted to produce the electron density peak at the correct altitude and the production coefficient is adjusted to give the correct magnitude in intensity at the peak.

As the incident intensities of the various wavelength bands change with time, the amplitude as well as the shape of the layers change. By monitoring the energy in the five wavelength bands with satellite instrumentation a real time predictive capability is built into the model. The slow variation of the atmospheric density model (caused by the slower heating effects) is coupled with the rapid response to changes in the ionizing radiation.

Figure 4 is a sample altitude profile plot which combines the effects of the various wavelengths to produce a smoothly varying density profile.

2.2.2 The F_2 Layer

The structure and variability in the F_2 layer is not so directly controlled by the neutral atmosphere. Attempts to treat the F_2 layer using U.V. generated ionization and electron losses which are a function only of density have ended in failure. It is generally agreed that the bottom of the F_2 layer is defined as the region where the electron loss rates change dramatically (from the order of seconds to the order of hours). Several studies were undertaken with neutral constituents and electron density dependent attachment and recombination coefficients. In none of these attempts was it possible to directly reproduce the observed seasonal, semi-annual or solar cycle dependencies.

An empirical function was therefore developed which arbitrarily (adjusted to provide a best fit at some point in time) defines a loss term varying with height and an ionization term depending only on the ambient density. Further empirical observations suggested that the normal F_2 layer was limited to the

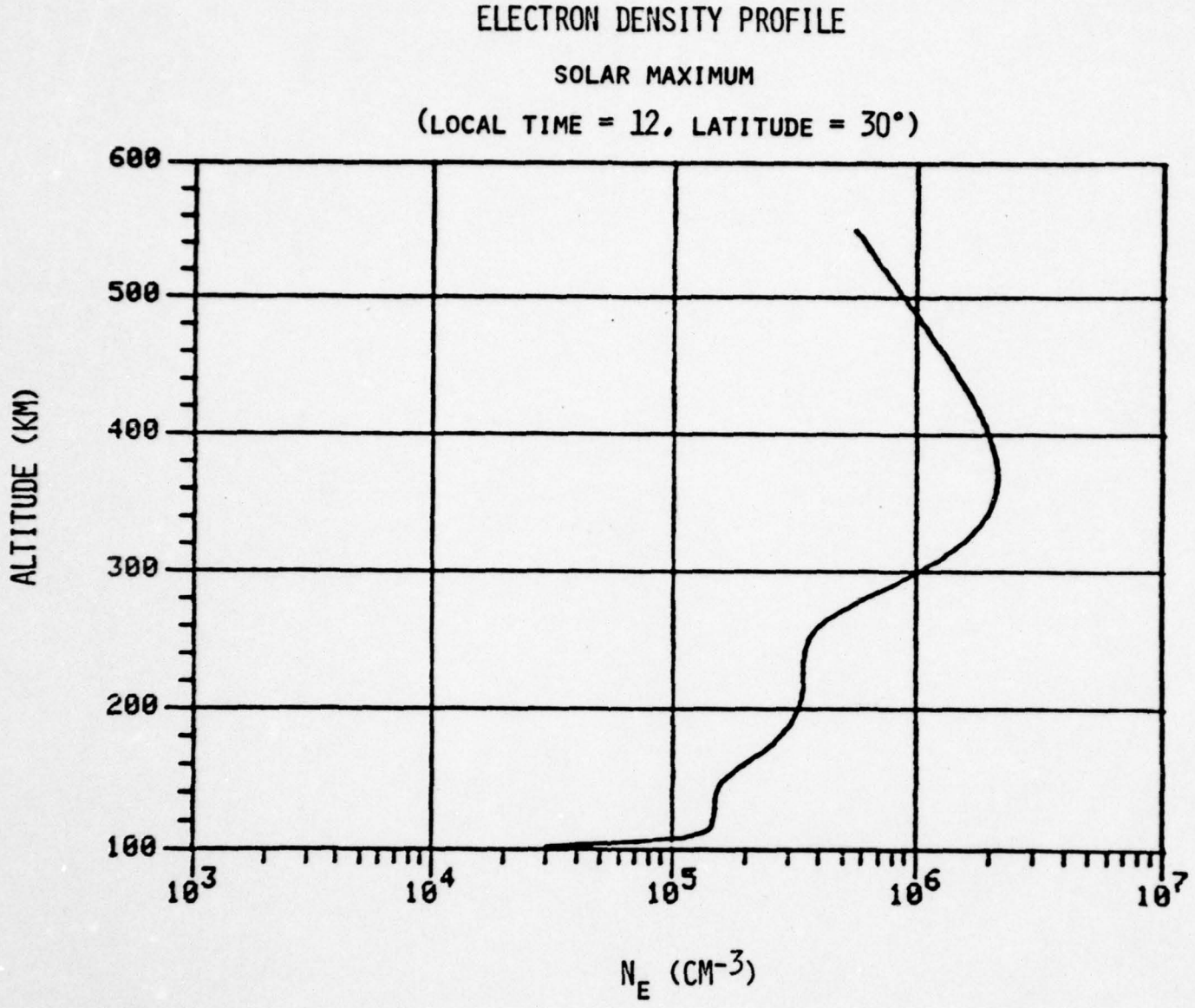
ELECTRON DENSITY PROFILE
SOLAR MAXIMUM
(LOCAL TIME = 12, LATITUDE = 30°)
ALTITUDE (KM)
600
500
400
300
200
100
10^3
10^4
10^5
10^6
10^7
N_E (CM^-3)

Figure 4.

region equatorward of the latitude of the plasmasphere. Thus, a function was introduced which limits the F_2 layer (except for the winter anomaly peak) to L values $\lesssim$ 4-6. (The L value can roughly be thought of as the equatorial extent of magnetic field lines measured from the center of the earth as given in earth radii. Thus at the equator L = 1.) That is, the neutral density dependent F_2 electron values are multiplied by the function.

$$G(\Lambda) = \exp(-\gamma \Lambda^3)$$

where $\Lambda = \cos^{-1}\left[\sqrt{\frac{1}{L}}\right]$ is the magnetic invariant latitude. The parameter γ was adjusted to give a best fit to the midnight equatorward edge of the mid latitude trough. Thus, the parameter γ is a primary parameter, since it is derived from the size of the plasmasphere. To properly <u>calibrate</u> the parameter γ simultaneous satellite measurements of the edge of the plasmapause and measurements of the size of the polar cap are required. (Note however that the model will provide the location and extent of the trough - that measurement is <u>not</u> a model input.)

The F_2 layer is essentially independent of direct solar zenith angle control, and depends instead on the density of the neutral atmosphere and the latitude extent of the plasmasphere. The winter anomaly, however, does appear to depend on solar zenith angle. It appears at sunrise and rapidly disappears at sunset. Much of the average structure of the F_2 region as given by the model, including the F_2 peak, is shown in Figures 5 and 6 in terms of the critical frequency (which relates directly to N_e). Note that on the noon meridian some of the

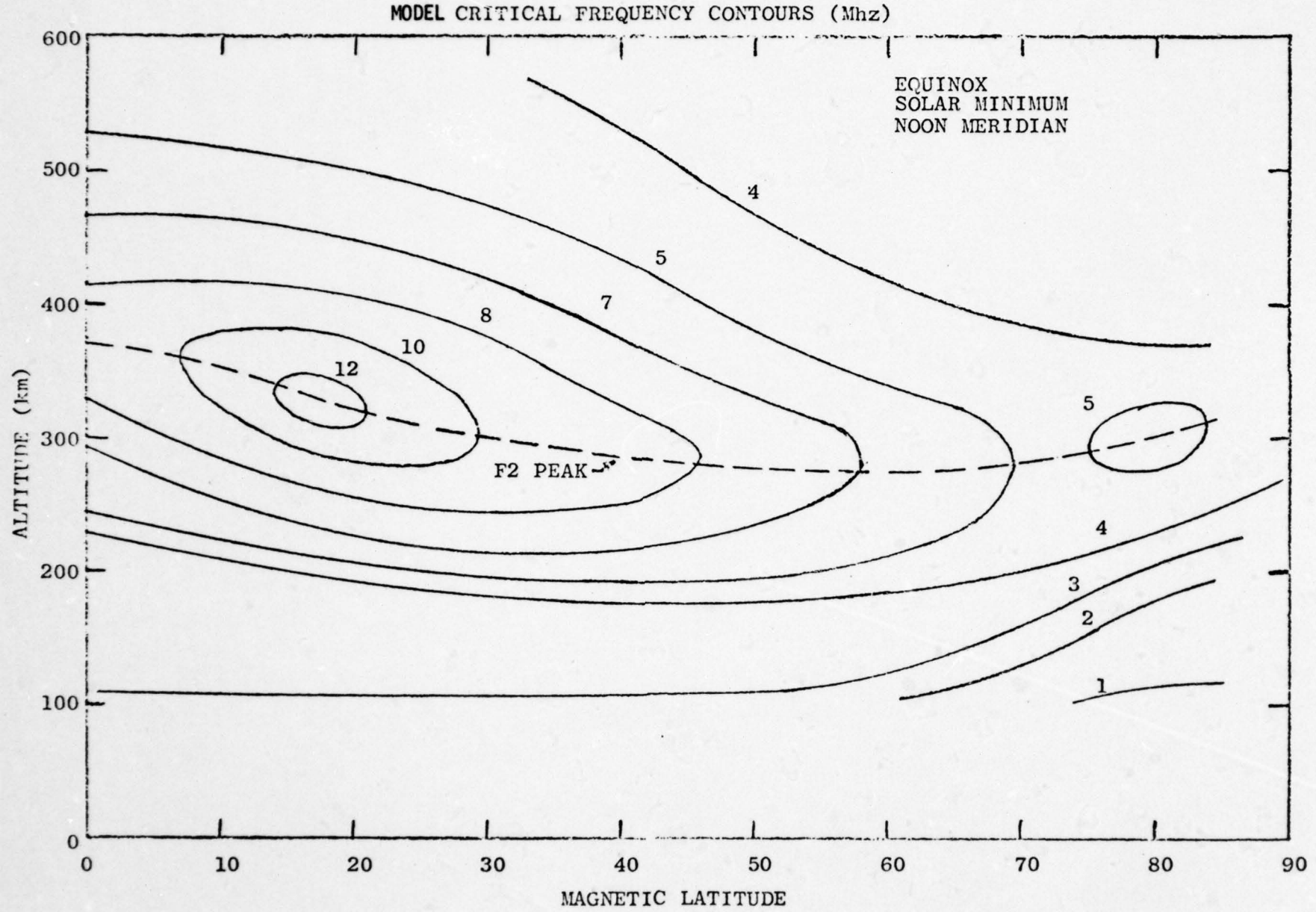
MODEL CRITICAL FREQUENCY CONTOURS (Mhz)
EQUINOX
SOLAR MINIMUM
NOON MERIDIAN
ALTITUDE (km)
MAGNETIC LATITUDE
F2 PEAK
12
10
8
7
5
4
5
4
3
2
1
600
500
400
300
200
100
0
0
10
20
30
40
50
60
70
80
90

Figure 5.

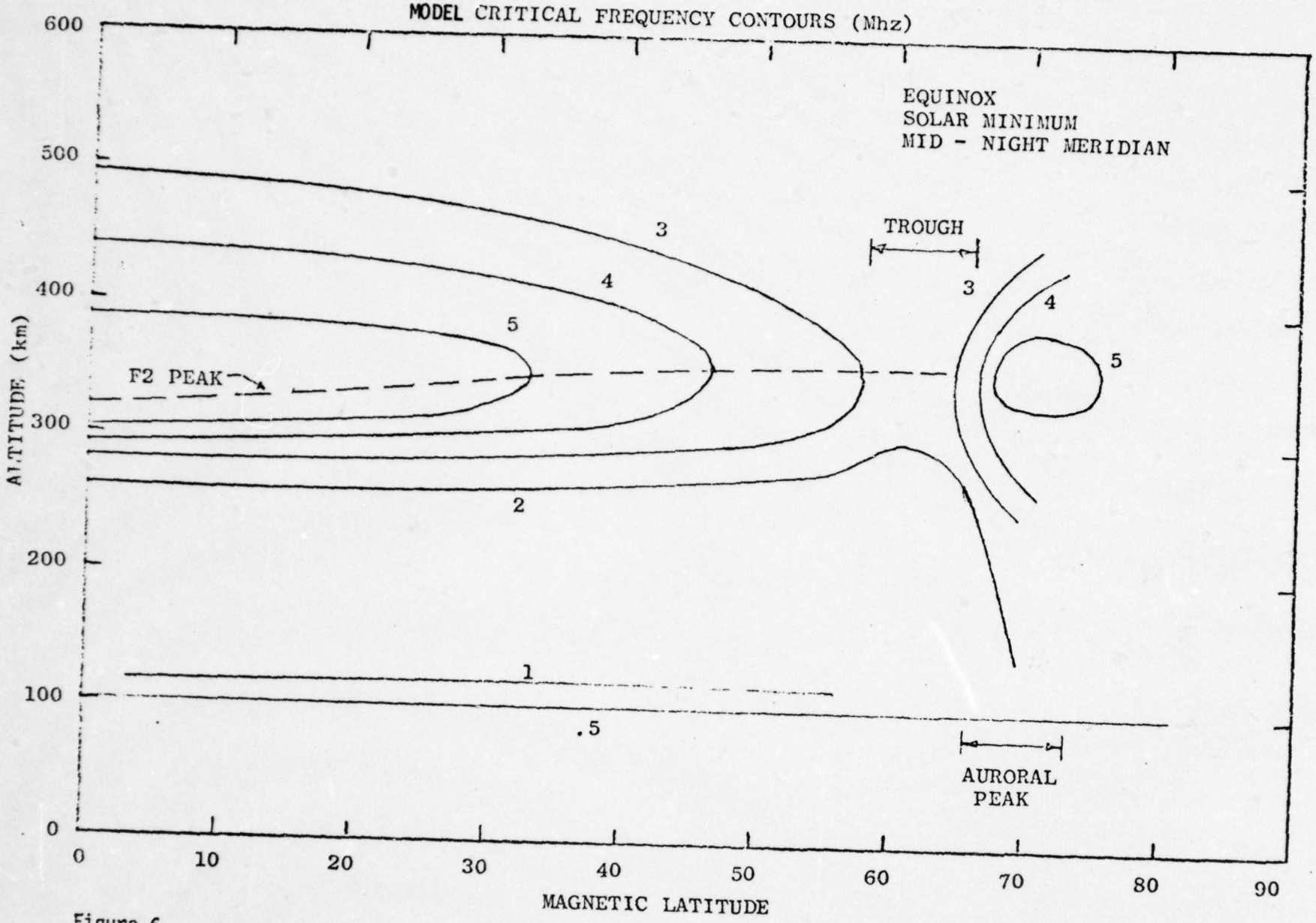
MODEL CRITICAL FREQUENCY CONTOURS (Mhz)
EQUINOX
SOLAR MINIMUM
MID - NIGHT MERIDIAN
TROUGH
F2 PEAK
AURORAL PEAK
ALTITUDE (km)
MAGNETIC LATITUDE
600
500
400
300
200
100
0
0
10
20
30
40
50
60
70
80
90
1
.5
2
3
4
5

Figure 6.

structure is produced by the equatorial anomaly (around the 12 Mhz contour). The magnetic latitude dependence of the equatorial anomaly is included in the model and is discussed below.

2.3 EQUATORIAL ANOMALY

The equatorial anomaly is thought to be caused by an upwelling of the ionosphere in the equatorial region produced by electric fields. It may be organized around a central L value, L_o. The functional form of the anomaly term is

$$d \cdot \exp\left[-\delta(L-L_o)^2\right]$$

where the amplitude, d, is dependent on solar cycle as well as local time and δ, which defines the width of the anomaly peaks, has a local time and solar cycle dependence and a latitude dependence. At a given altitude the equatorial anomaly is strongest along the magnetic field line with the L value, L_o (L_o = 1.13). Its dependence on altitude and magnetic latitude as given by the model are shown in Figure 7.

2.4 WINTER ANOMALY

In this model the winter anomaly is treated as having a completely separate source and its contribution to the electron content is assumed to be additive to all other electron sources. The formalism developed for the F_1 layer was also used to describe the electrons associated with the winter anomaly. The winter anomaly's contribution to the F_2 layer, $N_e^{F_{2W}}$, during the winter months near solar maximum is therefore written as

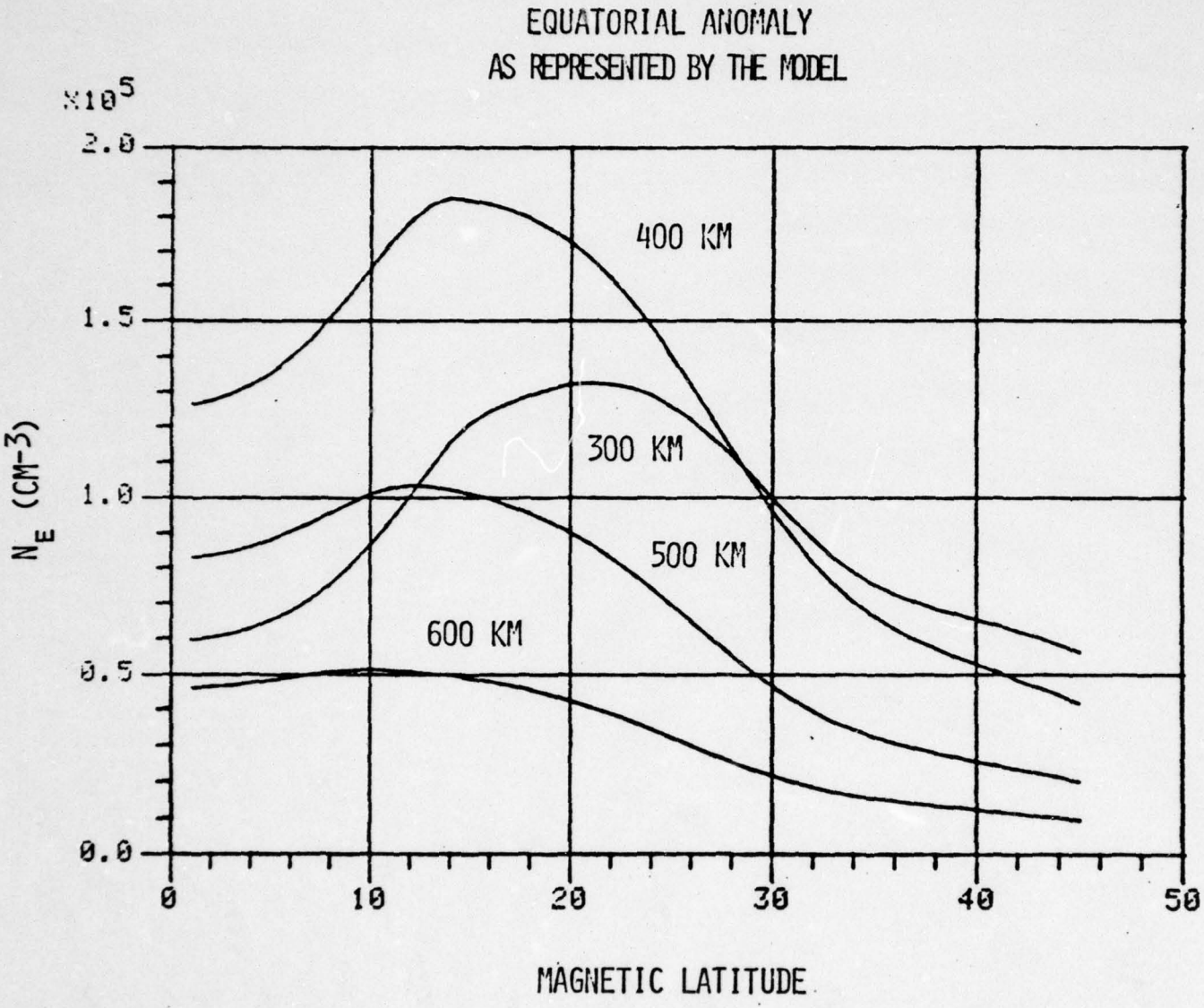
EQUATORIAL ANOMALY
AS REPRESENTED BY THE MODEL
X10^5
2.0
1.5
1.0
0.5
0.0
N_E (CM-3)
400 KM
300 KM
500 KM
600 KM
0
10
20
30
40
50
MAGNETIC LATITUDE

Figure 7.

$$N_e^{F_{2W}} = g(\lambda,\rho)\ [NS_{F_{2W}}\ \alpha_{F_{2W}}\ \exp(-\tau_{F_{2W}})]^{1/2}$$

where $g(\lambda,\rho)$ is a latitude and solar cycle dependent function which determines the extent and amplitude of the winter anomaly. N is the neutral density, $S_{F_{2W}}$ is the solar flux responsible for the ionization, $\alpha_{F_{2W}}$ is the ionization efficiency, and $\tau_{F_{2W}} = \sigma_{F_{2W}}\ T$, where $\sigma_{F_{2W}}$ is the absorption coefficient and T the optical density to the sun.

In general there is no F_2 layer over the polar cap in the above formulation (except for the winter anomaly which at times extends into the polar cap). The F_1 layer, however, extends to higher and higher altitudes as the light-dark terminator is reached.

2.5 POLAR CAP STRUCTURE AND MID-LATITUDE TROUGH

To complete the polar cap structure the charged particle source must be included. These high latitude sources appear most often at auroral latitudes (at L values greater than 8.5-9). At night the particles originate from the tail and are more energetic than the particles which continuously precipitate through the dayside cusp regions.

The configurations of the auroral E and F layers vary extensively in amplitude and location. For sake of simplicity a simple Gaussian in latitude has been used centered at L = 10.5 with a low latitude edge of 8.5 at midnight. During daylight hours the low latitude edge moves to slightly higher latitudes and is centered on the dayside cusp field line.

The disappearance of the F_2 plasmasphere associated electron density (at latitudes above the field lines passing through the plasmapause) together with the corpuscular generated auroral electron layer forms the midlatitude trough. During daylight hours, especially during the winter, the U.V. produced electron concentration may "fill in" the trough. The variation in the F_2 peak through the trough region is shown for the "average" model in Figure 8. Note that this important feature in N_e is largely under magnetic control. That is, as the plasmasphere expands or contracts, the low latitude edge of the trough moves respectively to higher or lower latitudes. Likewise the field lines along which the dayside cusp particles precipitate can also change their latitude and simultaneously the latitude of the poleward edge of the trough. The comparison between model and observations of the motion and extent of the midlatitude trough should be one of the first quantitative tests made of the model.

2.6 SAMPLE MODEL RESULTS

The model has been "calibrated" using average relative values of the electromagnetic flux to produce average profiles. Some of these profiles for the spring equinox are shown in Figures 9 through 13. Plots 9 to 11 show the noon time density profiles for various latitudes at solar minimum. Plots 12 and 13 are examples for solar maximum.

In order to better represent the seasonal and solar cycle dependence, plots of the critical frequency for each layer versus time have been generated. On these plots DAY = 0 represents January 1 at solar minimum. The electromagnetic flux is then allowed to change in a sinusoidal manner over an eleven year cycle.

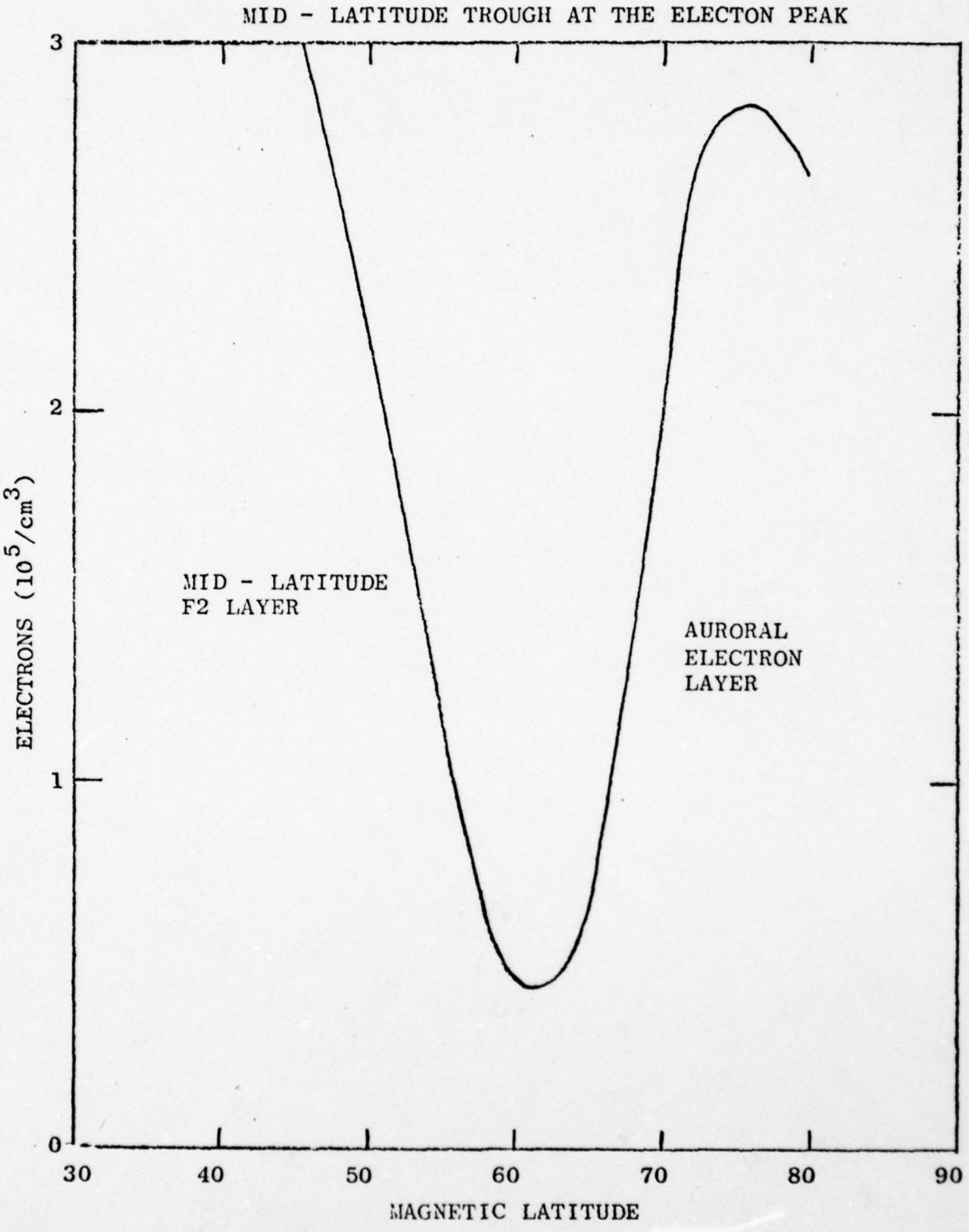
MID - LATITUDE TROUGH AT THE ELECTON PEAK
3
2
1
0
ELECTRONS (10^5/cm^3)
MID - LATITUDE
F2 LAYER
AURORAL
ELECTRON
LAYER
30
40
50
60
70
80
90
MAGNETIC LATITUDE

Figure 8.

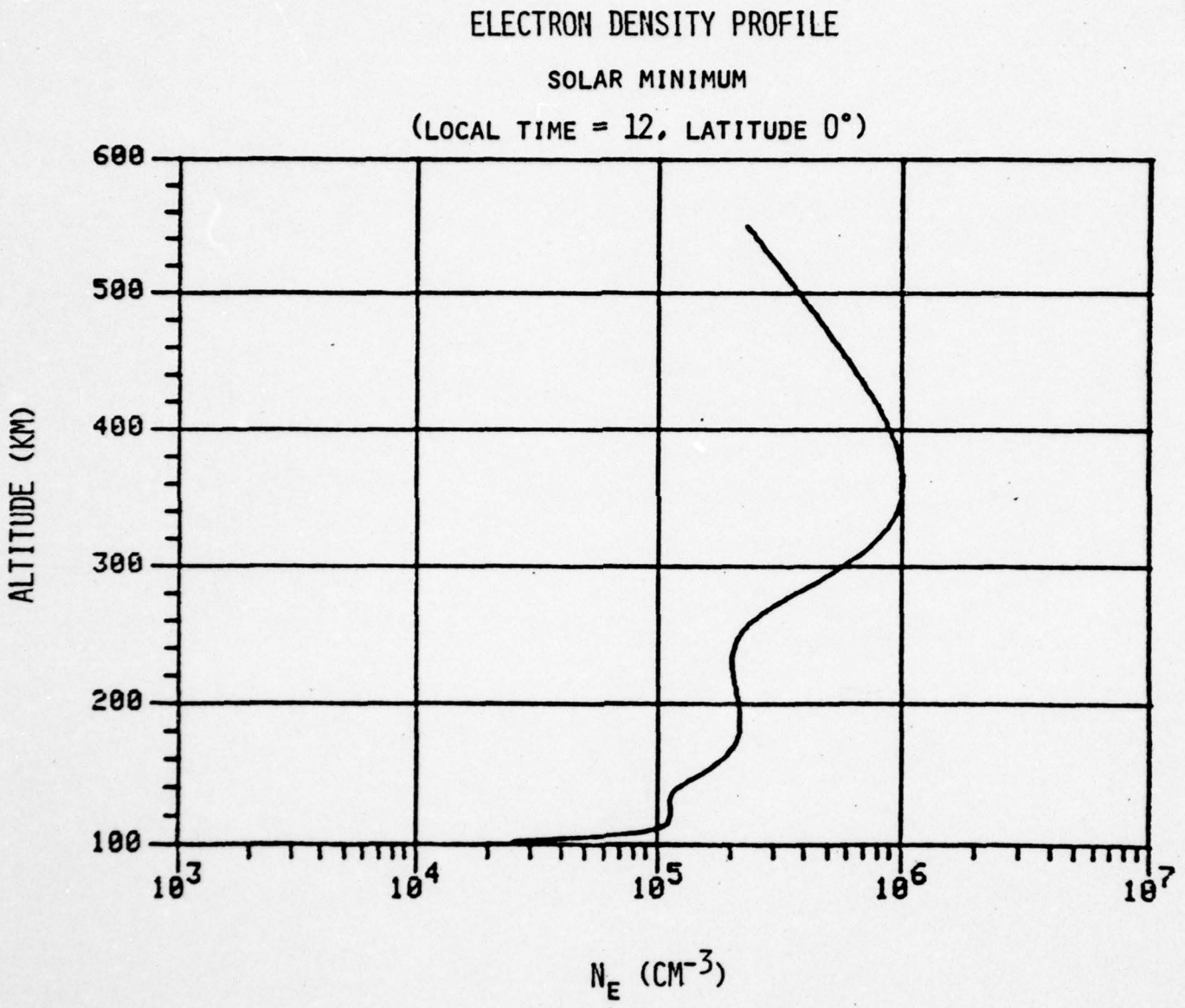
ELECTRON DENSITY PROFILE
SOLAR MINIMUM
(LOCAL TIME = 12, LATITUDE 0°)
ALTITUDE (KM)
600
500
400
300
200
100
10^3
10^4
10^5
10^6
10^7
N_E (CM^{-3})

Figure 9.

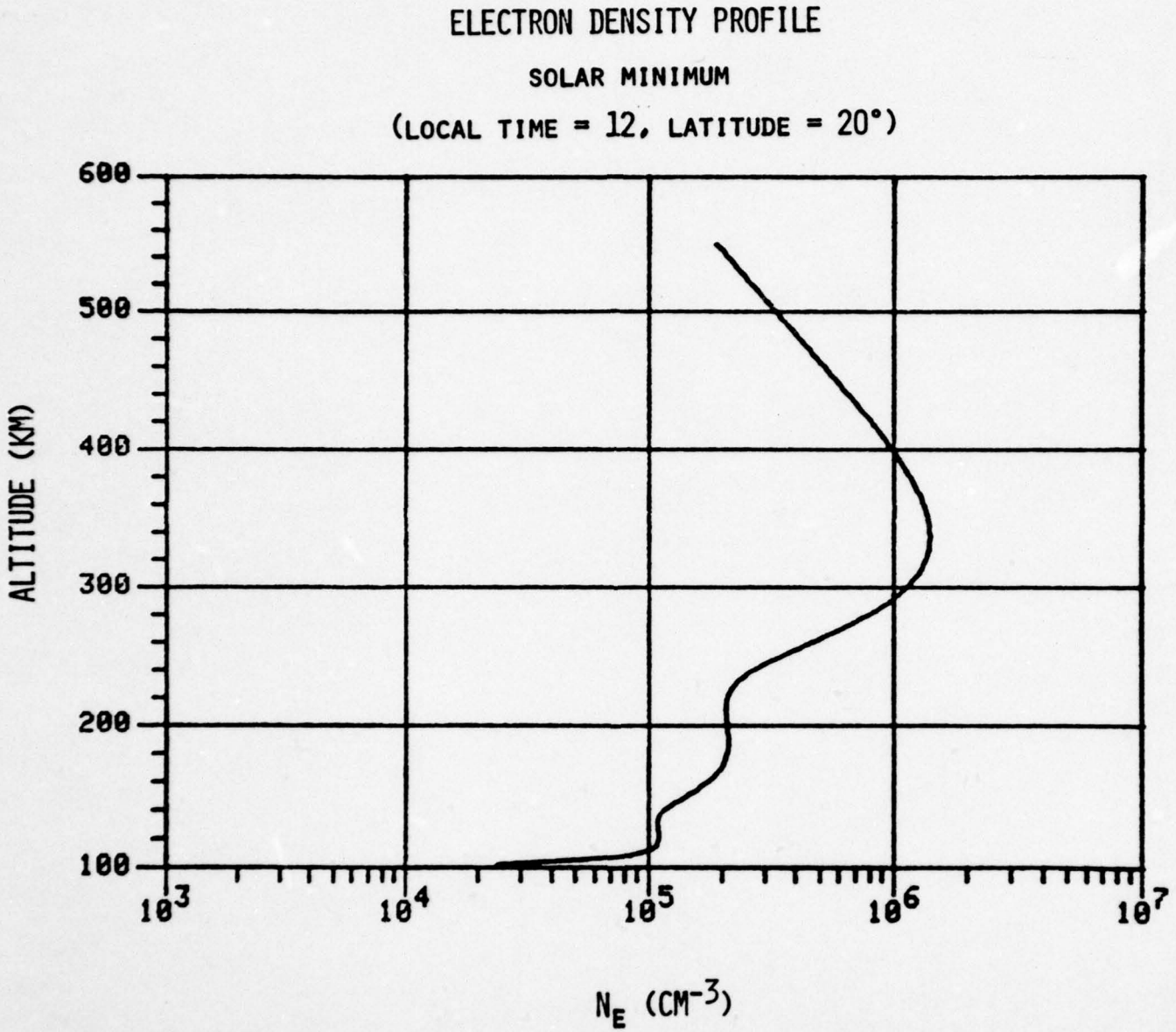
ELECTRON DENSITY PROFILE
SOLAR MINIMUM
(LOCAL TIME = 12, LATITUDE = 20°)
ALTITUDE (KM)
600
500
400
300
200
100
10^3
10^4
10^5
10^6
10^7
N_E (CM^{-3})

Figure 10.

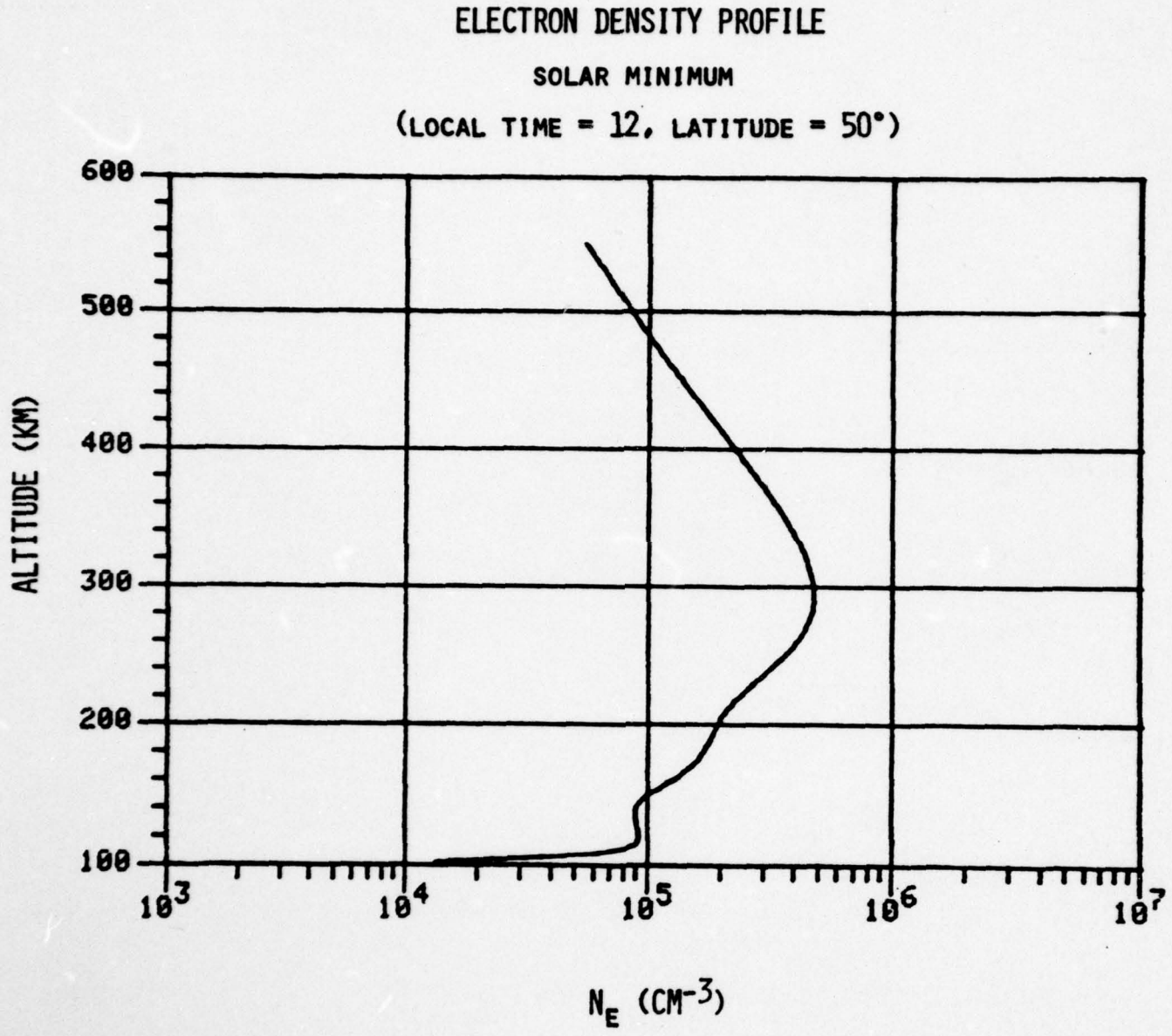
ELECTRON DENSITY PROFILE
SOLAR MINIMUM
(LOCAL TIME = 12, LATITUDE = 50°)
ALTITUDE (KM)
600
500
400
300
200
100
10^3
10^4
10^5
10^6
10^7
N_E (CM^{-3})

Figure 11.

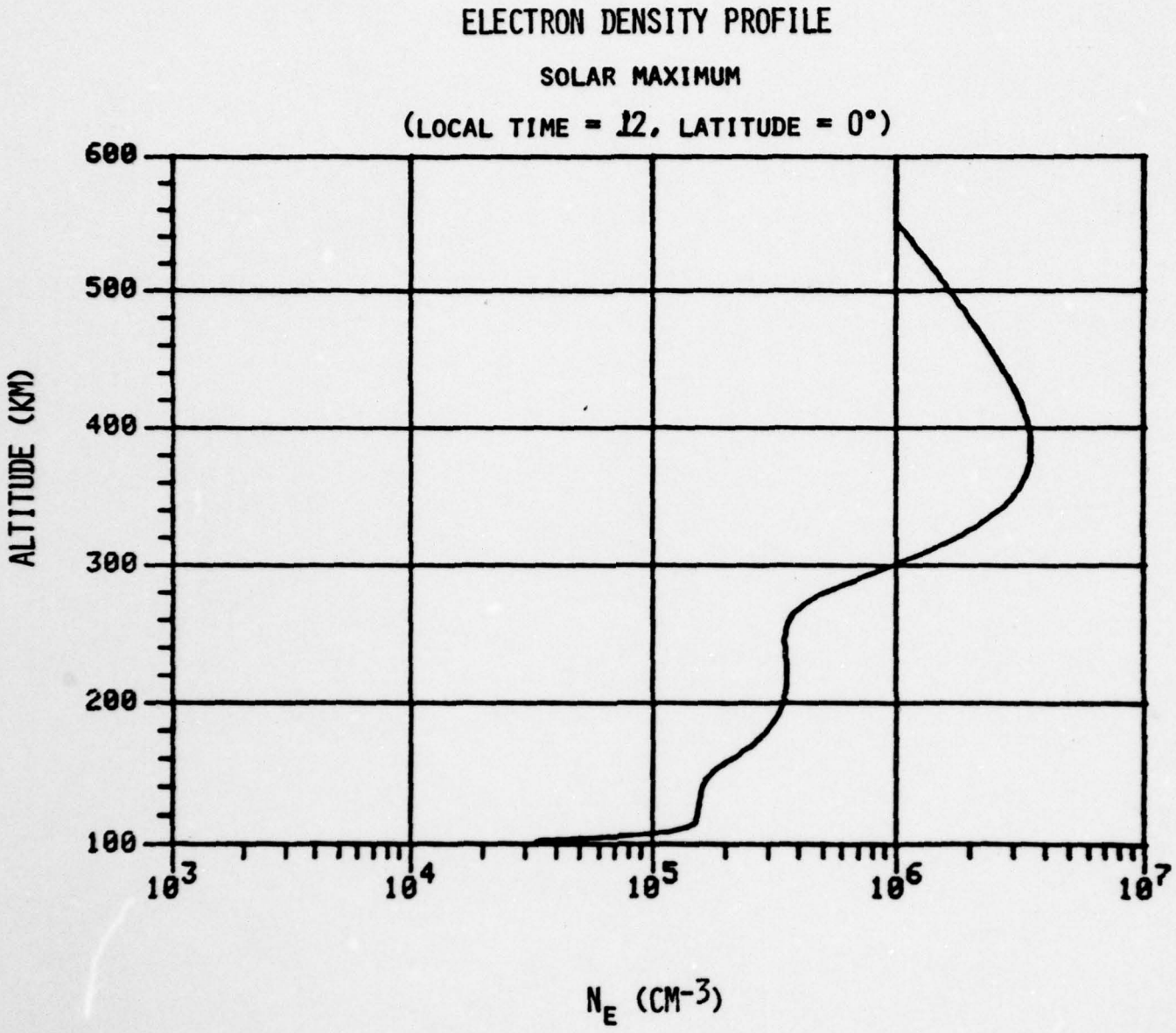
ELECTRON DENSITY PROFILE
SOLAR MAXIMUM
(LOCAL TIME = 12, LATITUDE = 0°)
ALTITUDE (KM)
600
500
400
300
200
100
10^3
10^4
10^5
10^6
10^7
N_E (CM^{-3})

Figure 12.

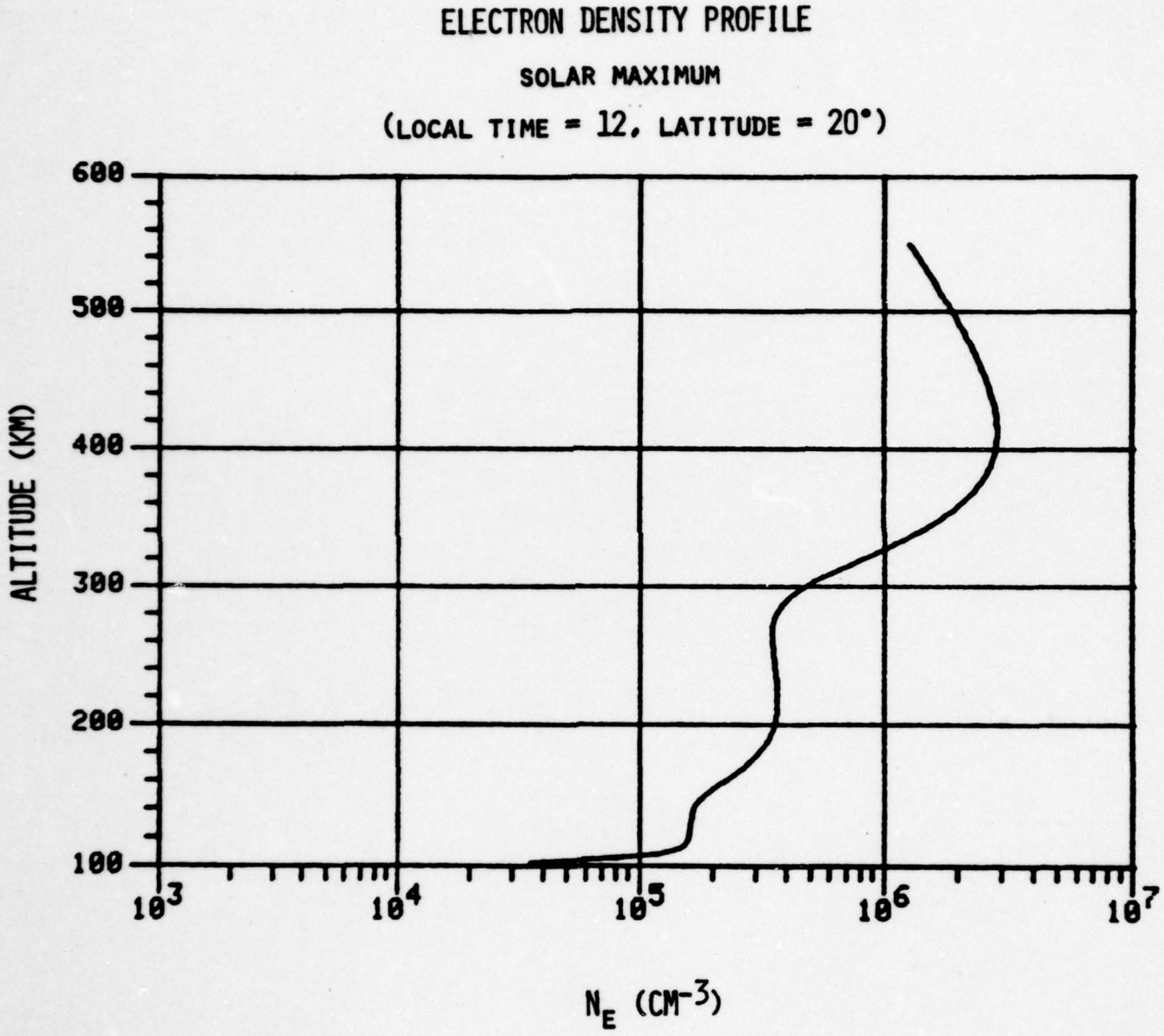
ELECTRON DENSITY PROFILE
SOLAR MAXIMUM
(LOCAL TIME = 12, LATITUDE = 20°)
ALTITUDE (KM)
600
500
400
300
200
100
10^3
10^4
10^5
10^6
10^7
N_E (CM^{-3})

Figure 13.

Figures 14 to 18 show this solar cycle dependence for various latitudes. Note, for example, the differences between northern and southern latitudes. They are primarily due to the interference between the winter anomaly and the semiannual variation. The winter anomaly is hemisphere dependent while the semiannual variation is not. The observed noontime critical frequencies at Slough are compared with model calculations in Figure 19 and shown to be in good agreement.

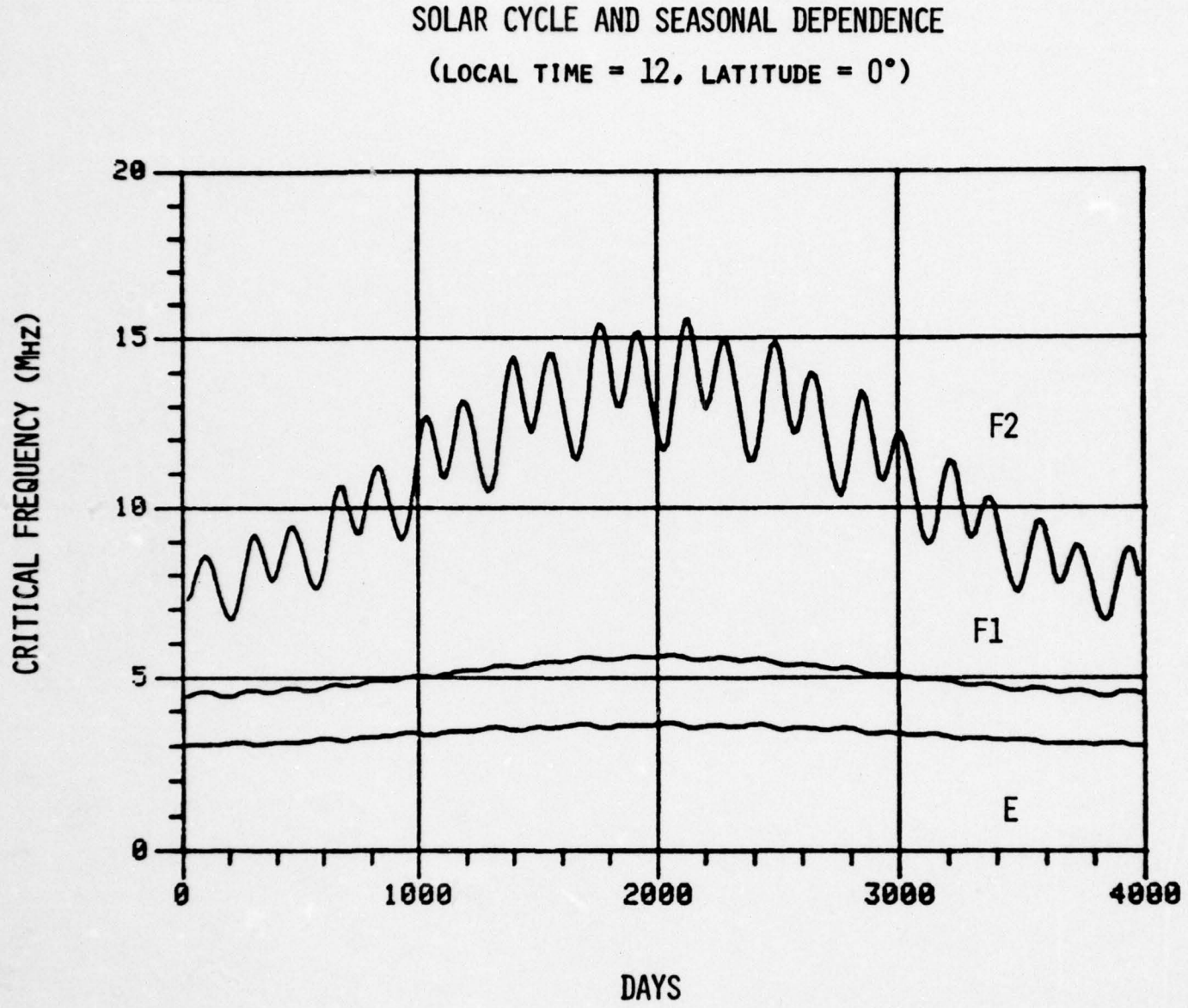
SOLAR CYCLE AND SEASONAL DEPENDENCE
(LOCAL TIME = 12, LATITUDE = 0°)
CRITICAL FREQUENCY (MHz)
20
15
10
5
0
F2
F1
E
0
1000
2000
3000
4000
DAYS

Figure 14.

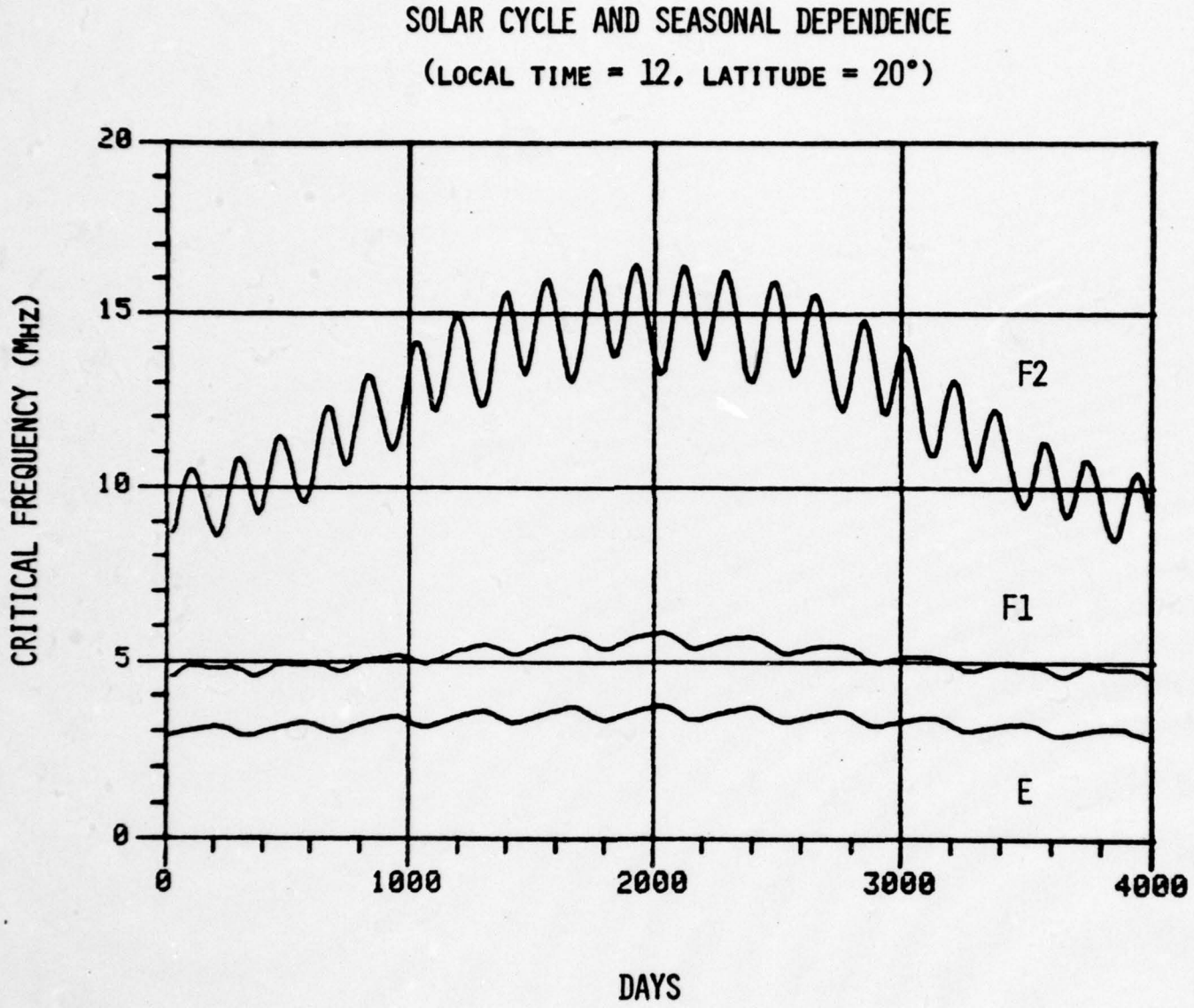
SOLAR CYCLE AND SEASONAL DEPENDENCE
(LOCAL TIME = 12, LATITUDE = 20°)
CRITICAL FREQUENCY (MHz)
20
15
10
5
0
F2
F1
E
0
1000
2000
3000
4000
DAYS

Figure 15.

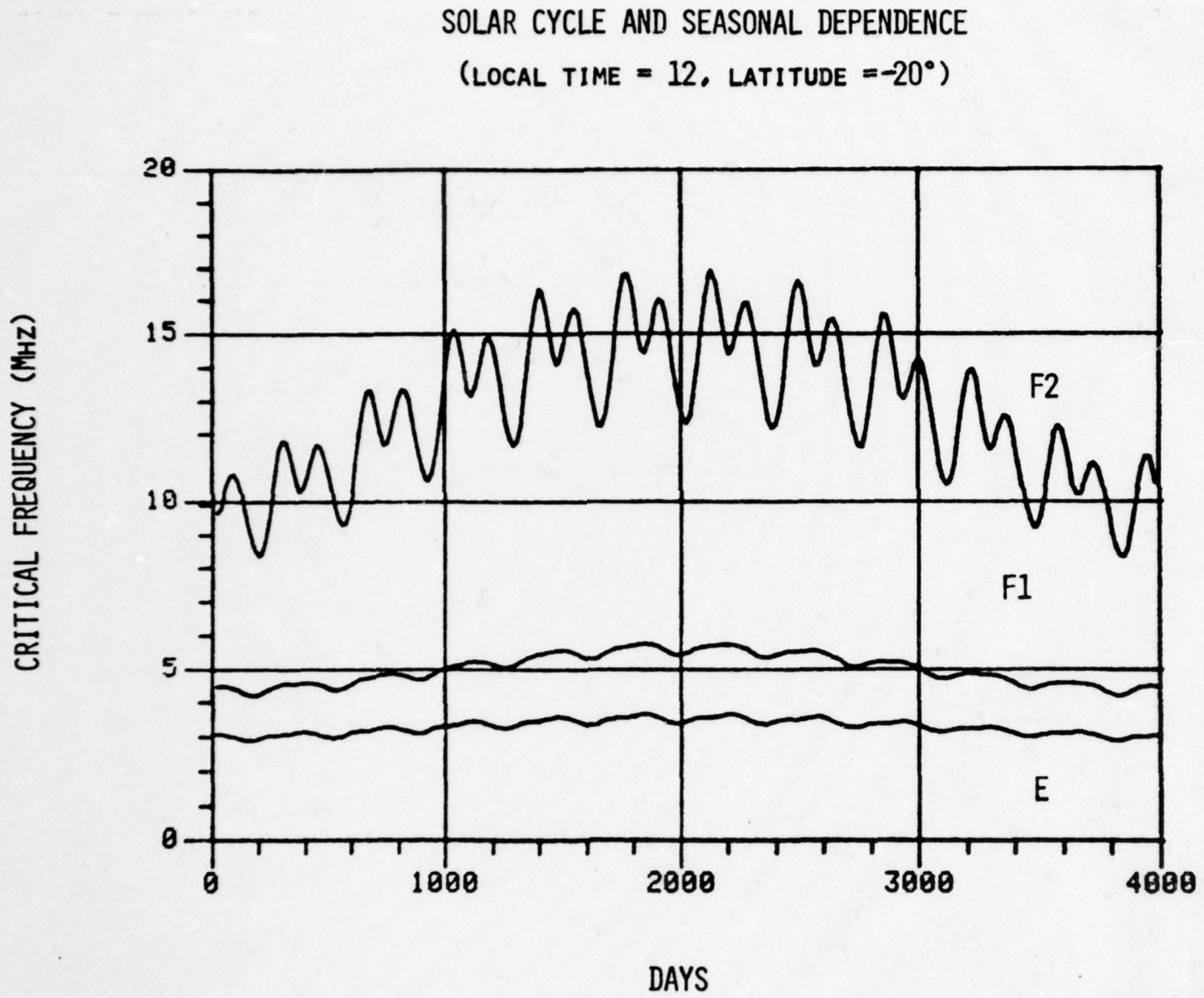
SOLAR CYCLE AND SEASONAL DEPENDENCE
(LOCAL TIME = 12, LATITUDE =-20°)
CRITICAL FREQUENCY (MHz)
20
15
10
5
0
F2
F1
E
0
1000
2000
3000
4000
DAYS

Figure 16.

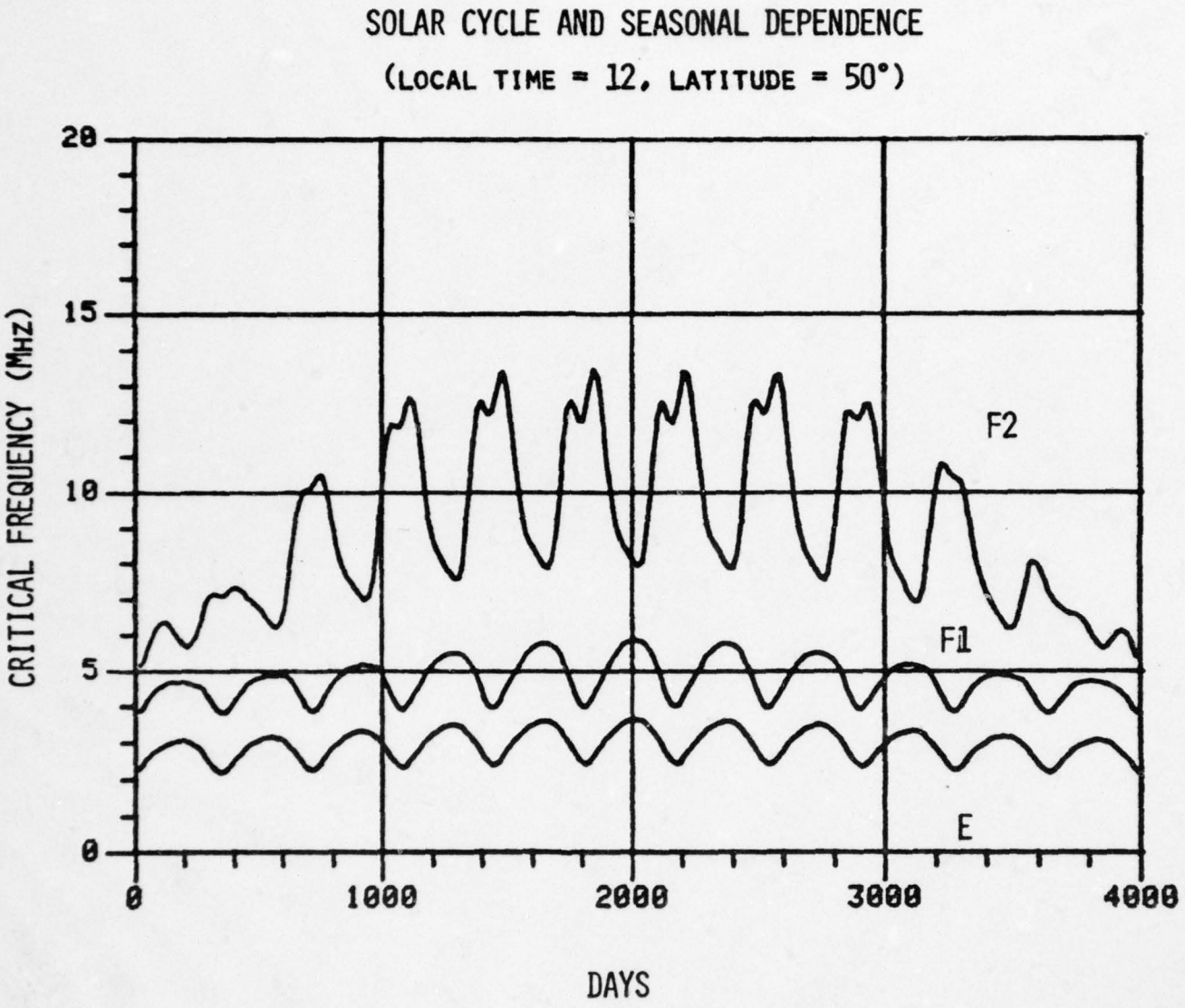
SOLAR CYCLE AND SEASONAL DEPENDENCE
(LOCAL TIME = 12, LATITUDE = 50°)
CRITICAL FREQUENCY (MHz)
20
15
10
5
0
F2
F1
E
0
1000
2000
3000
4000
DAYS

Figure 17.

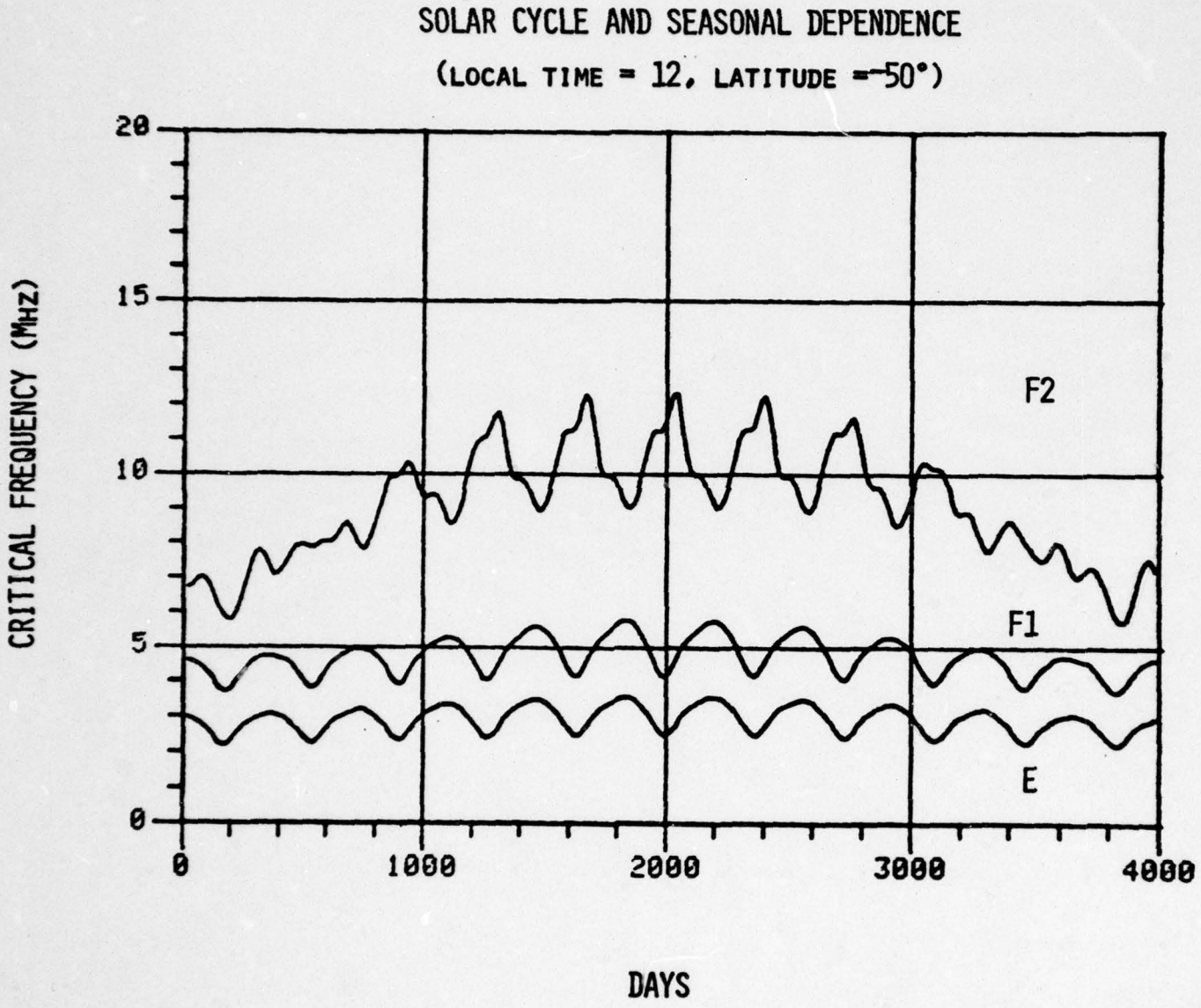
SOLAR CYCLE AND SEASONAL DEPENDENCE
(LOCAL TIME = 12, LATITUDE = -50°)
CRITICAL FREQUENCY (MHz)
20
15
10
5
0
F2
F1
E
0
1000
2000
3000
4000
DAYS

Figure 18.

MONTHLY NOON CRITICAL FREQUENCIES AT SLOUGH,
1932-1962 (FIG. 3.19, K. DAVIES, 1966)

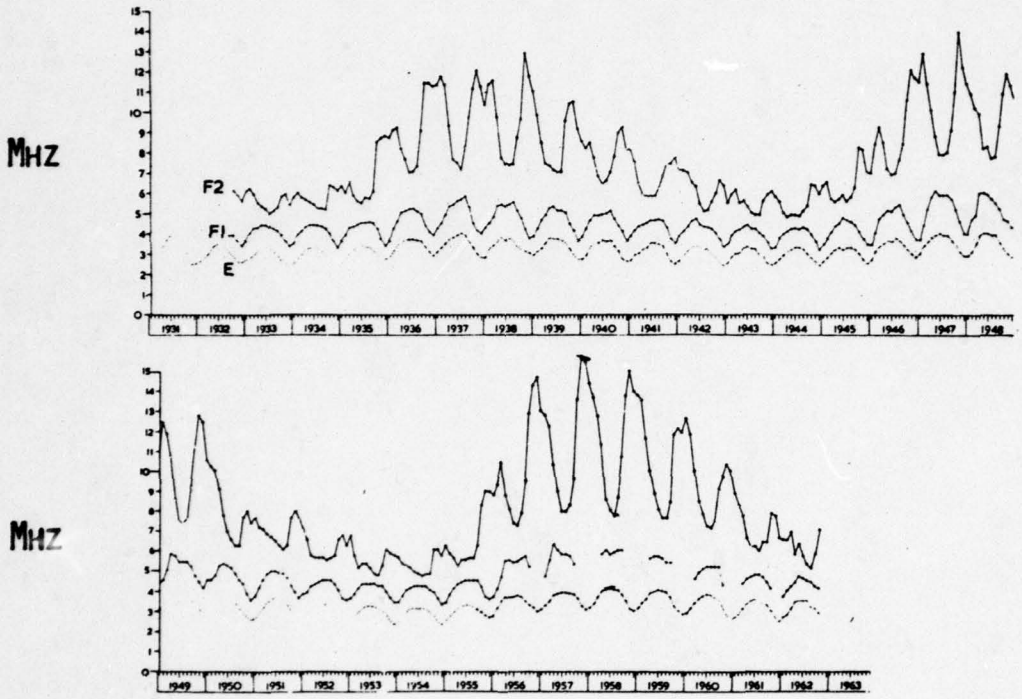

Figure 19.

Section 3.0

MODEL CALIBRATION

The description of the model in the previous section merely provides a glimpse at its "ground state." That is, the figures and data calculated from the model are based on "average" input parameters. We note that this average model already contains information on seasonal variations, dependence on solar cycle, and the necessary structure in latitude and altitude in order to accurately describe "quiet" features in N_e. We believe that even this average model can be of much value since it is global and has an associated fast computer code.

However, the purpose for the construction of this model was to provide a tool for the description of <u>variability</u> in N_e. This is only possible if the model possesses the proper input parameters <u>and</u> it is known how variations in each of the input parameters produce change in N_e. The model input parameters have been chosen so that if they are monitored in real time it will be possible to use the model to calculate changes in N_e. They include information on various bands in the solar electromagnetic energy spectrum, several data on the geomagnetic field, and a set of additional variables which describe other solar and interplanetary features.

Note that magnetic indicies such as K_p are not used. There are two reasons for this. First, such an index measures a quantity (the range in a component of the earth's surface magnetic field over a three hour interval at several polar observatories) that is controlled by many geophysical processes, making it difficult, if not impossible, to isolate causal relationships. Also, these indices are usually not available on a real time basis.

The input parameters used in the model then are chosen so that they can be monitored continuously by satellites such as SOLRAD-HI and the HELIOCENTRIC orbiter. In order to make the model "responsive" to these inputs it is necessary to calibrate it--to determine the response of the single model output, N_e, to changes in each of the input parameters. The calibration, of necessity, involves two types of data; those which describe variability in the input parameters, and proof data--those which can be used to check the calculated values of N_e with the observed values of N_e (associated with the given input parameter data).

The principal data sets to be used for this calibration are from the SOLRAD-HI satellite (to describe the input parameters) and other satellite data sets as available. The proof data will come mostly from ionograms. The ionosonde stations (latitude and longitude) will be chosen so that all of the day-night, latitudinal, and solar activity variations in the model can be calibrated. In agreement with the NRL people and NSF (which plays the role of US coordinator for the International Magnetospheric Study) we will concentrate on the month of September, 1977. During that month the current solar cycle began and there are periods of both quiet and moderately disturbed conditions. Also, the IMS has agreed that 6 days in 1977 will be analyzed in detail. Three of them are during the month of September. We therefore expect that in the next few months there will be a rather large amount of data available for analysis. The ionograms will be obtained from the World Data Center in Boulder. Their people tell us that our requests for ionograms can be honored in the next few months as they receive the ionosonde data from stations of interest to us.

Once calibrated, the model will hopefully be useful both for specifying gross features in N_e and for the actual prediction of some of them. Clearly the ionosphere responds quickly to changes in electromagnetic radiation from the sun and it is only possible to predict such changes by first predicting changes in solar surface features. There are however, several aspects of ionospheric behavior that are influenced by the geomagnetic field and the precipitation of charged particles into the upper atmosphere at auroral and polar latitudes. Such features respond to changes in interplanetary parameters such as the density and velocity of the solar wind and the polarity of the interplanetary magnetic field. These changes can be measured before they influence N_e. For such changes this model, when calibrated, should constitute a truely predictive tool.

Section 4.0

SUMMARY

A global model of the density of ionospheric electrons, N_e, has been developed. It is much faster as a computer code than any of the existing physical models. Also, it is not statistical but rather semiempirical. That is, a good deal of the model is based on physical understanding of ionospheric features but other portions are based on observational data. The model has been constructed such that it can be used in the prediction of the variability of N_e. It is intended that the model inputs are all based on data observed in real time rather than on any of the magnetic indices. The model can of course be used in other than real time settings and with minor modification used with magnetic indices as inputs. We expect that the model will be useful to the Navy in its continuing work on radio communications and that several research groups will find it helpful in such scientific studies as the understanding and description of the neutral wind problem (which takes as a starting point the densities of both the neutral atmosphere and N_e).

The calibration of the model with satellite and ionosonde data should be complete in the next several months and the model available for use by the end of the calendar year. We would be happy to hear any advice the readers of this report might forward to us.

Section 5.0

TECHNICAL REFERENCES

1. Bruce, R. W. Upper Atmosphere Density Determined from a Low-g Accelerometer on Satellite 1967-50B, Rep. TOR-0158 (3110-01) -16. Aerospace Corp., El Segundo, California. 1968.

2. Davies, K. Ionospheric Radio Propagation. Dover Publications. New York. 1966.